Mechanisms of Exchange Bias with Multiferroic $BiFeO_3$ Epitaxial Thin Films

H. Béa,[1] M. Bibes,[1] F. Ott,[2] B. Dupé,[1] X.-H. Zhu,[1] S. Petit,[2] S. Fusil,[1] C. Deranlot,[1]
K. Bouzehouane,[1] and A. Barthélémy[1,*]

[1]*Unité Mixte de Physique CNRS/Thales, Route départementale 128, 91767 Palaiseau, and Université Paris-Sud, 91405 Orsay, France*
[2]*Laboratoire Léon Brillouin CEA/CNRS UMR12, 91191 Gif sur Yvette, France*

(Received 6 September 2007; published 9 January 2008)

We have combined neutron scattering and piezoresponse force microscopy to show that the exchange field in CoFeB/$BiFeO_3$ heterostructures scales with the inverse of the ferroelectric and antiferromagnetic domain size of the $BiFeO_3$ films, as expected from Malozemoff's model of exchange bias extended to multiferroics. Accordingly, polarized neutron reflectometry reveals the presence of uncompensated spins in the $BiFeO_3$ film at the interface with CoFeB. In view of these results, we discuss possible strategies to switch the magnetization of a ferromagnet by an electric field using $BiFeO_3$.

DOI: 10.1103/PhysRevLett.100.017204 PACS numbers: 75.50.Ee, 75.70.Cn, 75.70.Kw, 77.80.−e

The renaissance of multiferroics [1,2], i.e., materials in which at least two ferroic or antiferroic orders coexist, is motivated by fundamental aspects as well as their possible application in spintronics [3]. Such compounds are rare and the very few that possess simultaneously a finite magnetization and polarization usually order below about 100 K [4–6]. Ferroelectric antiferromagnets (FEAF) are less scarce, and some exhibit a coupling between their two order parameters. This magnetoelectric (ME) coupling allows the reversal of the ferroelectric (FE) polarization by a magnetic field [7] or the control of the magnetic order parameter by an electric field [8].

The practical interest of conventional antiferromagnets (AF) is mainly for exchange bias in spin-valve structures. The phenomenon of exchange bias (EB) [9] manifests itself by a shift in the hysteresis loop of a ferromagnet (FM) in contact with an AF and arises from the exchange coupling at the FM/AF interface [10,11]. Combining this effect with the ME coupling in a FEAF/FM bilayer can allow the reversal of the FM magnetization via the application of an electric field through the FEAF, as reported recently at 2 K in $YMnO_3$/NiFe structures [12].

To exploit these functionalities in devices one needs to resort to FEAF materials with high transition temperatures. $BiFeO_3$ (BFO) is a FE perovskite with a Curie temperature of 1043 K [13] that orders antiferromagnetically below 643 K [14]. BFO thin films have a very low magnetization ($\sim 0.01 \mu_B$/Fe) compatible with an AF order [15,16], and remarkable FE properties with polarization values up to 100 $\mu C \cdot cm^{-2}$ [17]. Recently, we reported that BFO films can be used to induce an EB on adjacent CoFeB layers at 300 K [18]. This observation together with the demonstration of a coupling between the AF and FE domains [8] paves the way towards the room-temperature electrical control of magnetization with BFO. However, several questions remain before this can be achieved. Key issues concern the precise magnetic structure of BFO thin films and the mechanisms of EB in BFO-based heterostructures.

In this Letter, we report on the determination of the magnetic structure of BFO films by means of neutron diffraction (ND) and the analysis of the EB effect in CoFeB/BFO heterostructures in terms of Malozemoff's model [19]. Accordingly, we find a clear dependence of the amplitude of the exchange field H_E with the size of the multiferroic domains, which provides a handle to control the magnetization of the CoFeB film by an electric field. The observation of EB and enhanced coercivity correlates with the presence of uncompensated spins at the interface between the FM and the AF, as detected by polarized neutron reflectometry (PNR).

$BiFeO_3$ films were epitaxially grown by pulsed laser deposition [15], directly onto (001)- or (111)-oriented

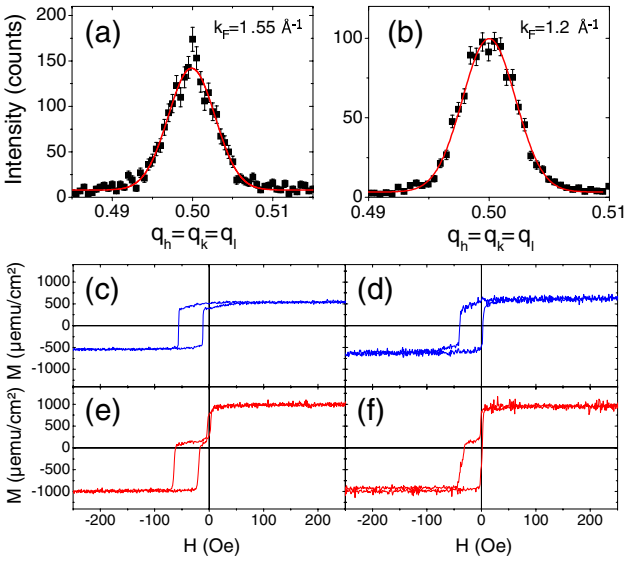

FIG. 1 (color online). (a), (b) Neutron diffraction scans close to the $[\frac{1}{2}\ \frac{1}{2}\ \frac{1}{2}]$ reflection for a 70 nm (001)- and a 300 nm (111)-oriented BFO films on STO, at 300 K. Magnetic field dependence of the magnetization of CoFeB/BFO(70 nm) (c), (d) and CoFeB/BFO(70 nm)/LSMO samples (e), (f) grown on (001)-oriented STO (c), (e) and (111)-oriented STO (d), (f), at 300 K.

$SrTiO_3$ (STO) or (001)-oriented $LaAlO_3$ (LAO) substrates, or onto 10–25 nm-thick metallic buffers of $La_{2/3}Sr_{1/3}MnO_3$ (LSMO) or $SrRuO_3$ (SRO) [20]. 7.5 nm-thick amorphous CoFeB layers were sputtered in a separate chamber at 300 K in a magnetic field of 200 Oe, after a short plasma cleaning. The samples were capped by 10–30 nm of Au. While the (111) films were found to be rhombohedral as bulk BFO [21], (001) films were found tetragonal or monoclinic [22].

A first key information that is usually required to analyze EB is the magnetic structure of the AF. Bulk BFO is known to have a G-type AF order [14], with a superimposed cycloidal modulation [23]. In view of the strong strain sensitivity of the properties of FE and magnetic oxides, one can anticipate that the magnetic order of BFO films might be different from that of the bulk. In order to determine their magnetic structure, selected (001)- and (111)-oriented BFO films were thus characterized by ND with the triple axis 4F1 spectrometer at the Orphée reactor of the Laboratoire Léon Brillouin (LLB).

In a G-type AF, superstructure peaks are expected to appear at $[\frac{1}{2}\ \frac{1}{2}\ \frac{1}{2}]$-type reflections. In Fig. 1(a) and 1(b), we show the diffracted intensity at the $[\frac{1}{2}\ \frac{1}{2}\ \frac{1}{2}]$ reflection in BFO films grown on (001)- and (111)-oriented STO. Clearly an AF peak is present for both films. No intensity was measured at $[0\ 0\ \frac{1}{2}]$-type or $[\frac{1}{2}\ \frac{1}{2}\ 0]$-type reflections, characteristic of A-type and C-type antiferromagnetism, respectively. This shows that both (001)- and (111)-oriented films are bulklike G-type AF. In other words, neither strain nor symmetry changes modify the type of magnetic order, besides destroying the cycloidal modulation [22].

Within a simplistic model of EB, the exchange field H_E depends on the interface coupling $J_{eb} = J_{ex}S_F S_{AF}/a^2$ (J_{ex} is the exchange parameter; S_F and S_{AF}, the spin of the interfacial atoms in the FM and the AF, respectively; and a the unit cell parameter of the AF), on the magnetization and thickness of the FM, M and t_F, and on the anisotropy K_{AF} and thickness t_{AF} of the AF as [11]:

$$H_E = \frac{-J_{eb}}{\mu_0 M t_F}\sqrt{1-\frac{J_{eb}^2}{4K_{AF}^2 t_{AF}^2}} = H_E^{\infty}\sqrt{1-\frac{1}{4\Re^2}}, \qquad (1)$$

provided that $1/4\Re^2$ is smaller than 1 (otherwise H_E is zero). If t_{AF} is large, $\Re \gg 1$ and $H_E \simeq H_E^{\infty}$. For perfect surfaces and because of the G-type AF order in both (001) and (111) films, the (111) films are expected to have magnetically uncompensated surfaces, yielding $S_{AF} = 5/2$, while the (001) films should have compensated surfaces, yielding in average $S_{AF} = 0$. Therefore, a large value $H_E = 6.5$ kOe should be found for (111) films only, taking $J_{ex} = 5 \times 10^{-22}$ J [24], $a = 3.96$ Å, $S_F = 1/2$, $S_{AF} = 5/2$, $M_{FM} = 800$ kA/m, and $t_{FM} = 7.5$ nm.

Figures 1(c) and 1(d) show $M(H)$ loops measured at 300 K for CoFeB/BFO(70 nm) stacks grown on STO(001) and STO(111). The loops are shifted towards negative magnetic field values by an exchange field H_E of -39 Oe for (001) films and -19 Oe for (111) films. Furthermore, the loops are enlarged by some tens of Oe compared to those measured on CoFeB single films [18]. From $M(H)$ data for CoFeB/BFO/LSMO samples [see Fig. 1(e) and 1(f)], a centered (not biased) contribution from the LSMO films is visible in addition to that coming from the CoFeB. For a given thickness, the exchange field experienced by the CoFeB is virtually the same irrespective of the presence of the LSMO buffer layer.

Malozemoff's random field model [19] has been proposed to resolve the long-standing discrepancy between the model of Eq. (1) and the experimental data [10]. It considers that in the presence of some atomic-scale disorder, that locally creates a net magnetization in the AF at the interface with the FM, the AF splits into domains, which decreases the interface coupling. Provided that $\Re \gg 1$, the exchange field is then given by [19]:

$$H_E = H_E^{\infty} = -\frac{J_{eb}}{\mu_0 M t_F} = -\frac{\zeta J_{ex} S_{AF} S_F}{\mu_0 M t_F a L}. \qquad (2)$$

L is the AF domain size and ζ a factor depending on the shape of the domains and on the average number z of frustrated interaction paths for each uncompensated surface spin. For hemispherical bubble domains, $\zeta \simeq 2z/\pi$ and z is of order unity. A variation of H_E as $1/L$ was indeed experimentally observed in several AF/FM systems [25,26], providing strong support to the model.

In order to determine the domain size in antiferromagnets, a technique of choice is x-ray photoelectron emission microscopy [27,28]. Alternatively, an estimation of the average domain size can be inferred from the width of the ND peaks that reflects the coherence length in the sample [22,29]. In some multiferroics like BFO, the FE and AF domains are coupled [8] so that it is possible to infer the size and distribution of the AF domains by imaging the FE domains, e.g., using piezoresponse force microscopy (PFM).

We have characterized the FE domains in two sets of BFO samples by combining in-plane and out-of-plane PFM measurements [30]. A first set consists of ~65 nm-thick BFO films grown on different buffers and substrates (see Table I). A second set consists of BFO films with varying thickness (5 nm $\leq t_{AF} \leq$ 240 nm) grown on LSMO//STO(001). In BFO, since the polarization is ori-

TABLE I. Experimental values of the exchange field and ferroelectric domain size for samples of the first set.

Substrate	Buffer	t_{AF} (nm)	H_E	L_{FE} (nm)
STO(001)	LSMO	70	−39	58
STO(001)	SRO	70	−14.5	98
STO(111)	LSMO	70	−19	68
STO(111)	SRO	70	−39	48
LAO(001)	LSMO	60	0	350
LAO(001)	SRO	60	−29	55

ented along the ⟨111⟩ directions there generally exist 8 possible polarization variants. This leads to several types of domain walls (DWs) depending on the angle between the polarization vectors in the adjacent domains (71°, 109°, or 180°). In principle only 71° and 109° FE DWs correspond to an AF DW [8]. In all samples the three types of DWs are present but the density of 180° type DWs is negligible.

In the following we analyze the exchange field in terms of the average FE domain size L_{FE} that we identify to half the FE domain periodicity and the average AF domain size L_{AF} that we identify to the coherence length in the ND experiments. Even in the case of a strict correspondence between the FE and AF domains, L_{FE} is expected to be larger than L_{AF} because it comprises both the domain and the DW widths while L_{AF} mostly reflects the domain width.

Let us first compare the values of L_{AF} and L_{FE} for the samples of Fig. 1. From Fig. 1(a) we calculate $L_{AF} = 42$ nm while from PFM we find $L_{FE} = 58$ nm for this sample. For the sample of Fig. 1(b), $L_{AF} = 56$ nm and $L_{FE} = 98$ nm. L_{FE} is larger than L_{AF} by some tens of nm that likely correspond to the DW width [31]. When L_{AF} increases L_{FE} increases also, as expected if the AF and FE domains are correlated, as found by Zhao *et al.* [8].

In Fig. 2(a) a linear variation of the exchange field with the inverse of the domain size is observed for the first set of samples, as expected from Eq. (2). Furthermore, there is an excellent *quantitative* agreement between the model and the data as visible from the similarity between the experimental points [solid symbols in Fig. 2(a)] and the values of H_E calculated using the domain sizes (open symbols; the best fit is obtained for $\zeta = 3.2$).

As illustrated by Fig. 2(b), this model also accounts for the thickness dependence of the exchange field. Below a critical BFO thickness of about 10 nm, there is no exchange bias but at larger thickness, $|H_E|$ increases abruptly and takes values of about 40 Oe for $t_{AF} \geq 35$ nm. A similar thickness dependence was reported for other AF/FM systems such as FeMn/NiFe [32] and is expected from Eq. (1). Combining Eq. (1) and the measured domain sizes one can calculate H_E for these films. The only free parameters are ζ and K_{AF}. As shown by the open symbols in Fig. 2(b), a rather good agreement with the data is obtained for $\zeta = 3.2$ and $K_{AF} = 6.8$ kJ/m^3. We note that this value of K_{AF} is lower than the value inferred for the bulk [24] but agrees well with data on $Bi_{0.9}Nd_{0.1}FeO_3$ films [33]. This can be due to the low thickness of the BFO films or to strain effects. This may also reflect modified magnetic properties at the CoFeB/BFO interface, as discussed in the following.

To validate the analysis of our data with Malozemoff's model, we have attempted to detect the presence of a net magnetization in BFO close to the interface with CoFeB using PNR. The PNR measurements were carried out with the PRISM instrument of the LLB at room temperature. Spin-up and spin-down reflectivities (R_{++} and R_{--}) were collected and the data were corrected for the polarization efficiency. The least square fittings were made using the Simul-Reflec software. The structural parameters of the layers were first determined by fitting x-ray reflectometry data (not shown). The studied sample, Au (31.0 ± 0.5 nm)/CoFeB (7.0 ± 0.5 nm)/BFO (18 ± 0.5 nm), displaying a CoFeB/BFO interface roughness of only 0.5 nm, shows an EB of −18 Oe.

Figure 3 shows the PNR results for this sample and the corresponding fits using two different sample models. In the first one [Fig. 3(a)] we only consider the presence of three layers, i.e., Au, CoFeB, and BFO. The best fit is obtained for the structure Au (31.0 ± 0.5 nm)/CoFeB (7.0 ± 0.5 nm)/BFO (18 ± 0.5 nm) with zero magnetization in BFO and Au, and a magnetization of 1 ± 0.05 μ_B/f.u. in CoFeB. The fit quality could be improved, especially at

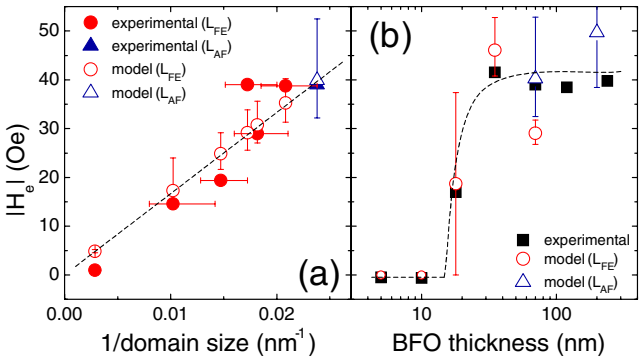

FIG. 2 (color online). (a) Dependence of the exchange field on the inverse of the domain size for several ~65 nm BFO films. (b) Thickness dependence of the exchange field for CoFeB/BFO stacks grown on STO(001). The dotted lines are guides to the eye.

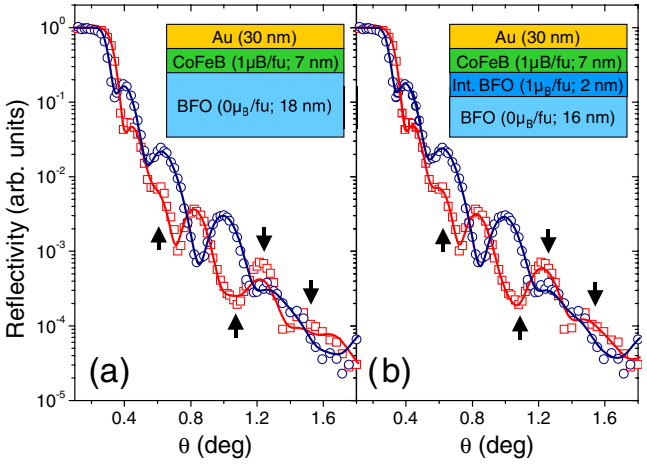

FIG. 3 (color online). Polarized neutron reflectivity data measured in a saturating field of 1.2 T (R_{++}: squares; R_{--}: circles) fitted with a three-layer model (a) and a four-layer model (b). Introducing an interface layer of ~2 nm carrying a moment of 1 ± 0.5 μ_B/f.u. significantly improves the quality of the fit for up-up reflectivity (see arrows).

high θ (see arrows), by adding an interfacial BFO layer [see inset of Fig. 3(b)]. The best fit is then obtained if a 2 ± 0.5 nm layer carrying a magnetic moment of $1 \pm 0.5\ \mu_B$/f.u. is present in this interfacial BFO layer. This layer accounts for the presence of a large density of uncompensated spins (corresponding to a surface moment $m_s = 31.8\ \mu_B \cdot \mathrm{nm}^{-2}$) at the CoFeB/BFO interface, as observed in $Co/LaFeO_3$ [34]. The magnetic order in BFO is thus different at the interface compared to the inner part of the film.

The expected surface moment due to pinned uncompensated spins within Malozemoff's model is $m_s^{\mathrm{pin}} = 2S_{\mathrm{AF}}/aL \simeq 0.32\ \mu_B \cdot \mathrm{nm}^{-2}$, which represents only 1% of the surface moment measured by PNR. The majority of uncompensated spins is thus unpinned (as observed in Co/IrMn [35]) and rotates with the CoFeB, producing an increase of the coercive field (see Fig. 1). This observation suggests that two different, yet possibly related and complementary, strategies are possible to tune the magnetic switching fields of the ferromagnet electrically. One would rely on the manipulation of the pinned uncompensated spins to modify H_E, e.g., by changing the domain size that should be controllable by *ad hoc* electrical writing procedures. The other could consist in controlling the unpinned uncompensated spins in order to alter the coercive field. This might be achieved by modifying the effective surface anisotropy of the AF, for instance, by playing with the ferroelastic energy of the domains, which would change the magnetoelastic contribution to the anisotropy.

In summary, we analyzed the exchange bias in the $CoFeB/BiFeO_3$ system and found that the exchange field scales with the inverse of the ferroelectric and antiferromagnetic domain size in (001)- and (111)-oriented multiferroic $BiFeO_3$ films, as expected from Malozemoff's model that we extend for the first time to the case of ferroelectric antiferromagnets. Polarized neutron reflectometry measurements reveal the presence of a net magnetic moment within a $\sim$2 nm slab in the BFO at the interface with the CoFeB, reflecting the presence of uncompensated spins in the $BiFeO_3$, consistent with the observation of exchange bias and enhanced coercivity. As the ferroelectric domain structure can be easily controlled by an electric field, our results strongly suggest that the electrical manipulation of magnetization should be feasible at room temperature in BFO-based exchange-bias heterostructures.

We acknowledge support by the EU STREP MACOMUFI (033221), the ANR-FEMMES, and the Conseil Général de l'Essone (H. B.). The authors would like to thank H. Jaffrès, M. Viret, G. Catalan, and J. Scott for fruitful discussions.

*agnes.barthelemy@thalesgroup.com

[1] N. Spaldin and M. Fiebig, Science **309**, 391 (2005).
[2] W. Eerenstein, N. D. Mathur, and J. F. Scott, Nature (London) **442**, 759 (2006).
[3] M. Bibes and A. Barthélémy, IEEE Trans. Electron Devices **54**, 1003 (2007).
[4] K. Kato and S. Iida, J. Phys. Soc. Jpn. **51**, 1335 (1982).
[5] Y. Yamasaki *et al.*, Phys. Rev. Lett. **96**, 207204 (2006).
[6] M. Gajek *et al.*, Nat. Mater. **6**, 296 (2007).
[7] T. Kimura *et al.*, Nature (London) **426**, 55 (2003).
[8] T. Zhao *et al.*, Nat. Mater. **5**, 823 (2006).
[9] W. H. Meiklejohn and C. P. Bean, Phys. Rev. **102**, 1413 (1956).
[10] J. Nogués and I. K. Schuller, J. Magn. Magn. Mater. **192**, 203 (1999).
[11] F. Radu and H. Zabel, arXiv:0705.2055.
[12] V. Laukhin *et al.*, Phys. Rev. Lett. **97**, 227201 (2006).
[13] J. R. Teague, R. Gerson, and W. J. James, Solid State Commun. **8**, 1073 (1970).
[14] S. V. Kiselev, R. P. Ozerov, and G. S. Zhdanov, Sov. Phys. Dokl. **7**, 742 (1963).
[15] H. Béa *et al.*, Appl. Phys. Lett. **87**, 072508 (2005).
[16] H. Béa *et al.*, Phys. Rev. B **74**, 020101(R) (2006).
[17] D. Lebeugle *et al.*, Appl. Phys. Lett. **91**, 022907 (2007).
[18] H. Béa *et al.*, Appl. Phys. Lett. **89**, 242114 (2006).
[19] A. P. Malozemoff, Phys. Rev. B **35**, 3679 (1987).
[20] H. Béa *et al.*, Appl. Phys. Lett. **88**, 062502 (2006).
[21] H. Béa *et al.* (unpublished).
[22] H. Béa *et al.*, Philos. Mag. Lett. **87**, 165 (2007).
[23] I. Sosnowksa, T. Peterlin-Neumaier, and E. Steichele, J. Phys. C **15**, 4835 (1982).
[24] B. Ruette *et al.*, Phys. Rev. B **69**, 064114 (2004).
[25] K. Takano *et al.*, Phys. Rev. Lett. **79**, 1130 (1997).
[26] A. Scholl *et al.*, Appl. Phys. Lett. **85**, 4085 (2004).
[27] J. Stöhr *et al.*, Phys. Rev. Lett. **83**, 1862 (1999).
[28] A. Scholl *et al.*, Science **287**, 1014 (2000).
[29] J. A. Borchers *et al.*, Appl. Phys. Lett. **77**, 4187 (2000).
[30] G. Catalan *et al.*, arXiv:0707.4377 [Phys. Rev. Lett. (to be published)].
[31] The width of DWs in BFO will be discussed elsewhere.
[32] R. Jungblut *et al.*, J. Appl. Phys. **75**, 6659 (1994).
[33] F. Huang *et al.*, Appl. Phys. Lett. **89**, 242914 (2006).
[34] A. Hoffmann *et al.*, Phys. Rev. B **66**, 220406(R) (2002).
[35] H. Ohldag *et al.*, Phys. Rev. Lett. **91**, 017203 (2003).